

Learning to Walk via Deep Reinforcement Learning

Tuomas Haarnoja^{1,2}, Aurick Zhou¹, Sehoon Ha², Jie Tan², George Tucker² and Sergey Levine^{1,2}

Abstract—Deep reinforcement learning suggests the promise of fully automated learning of robotic control policies that directly map sensory inputs to low-level actions. However, applying deep reinforcement learning methods on real-world robots is exceptionally difficult, due both to the sample complexity and, just as importantly, the sensitivity of such methods to hyperparameters. While hyperparameter tuning can be performed in parallel in simulated domains, it is usually impractical to tune hyperparameters directly on real-world robotic platforms, especially legged platforms like quadrupedal robots that can be damaged through extensive trial-and-error learning. In this paper, we develop a stable variant of the soft actor-critic deep reinforcement learning algorithm that requires minimal hyperparameter tuning, while also requiring only a modest number of trials to learn multilayer neural network policies. This algorithm is based on the framework of maximum entropy reinforcement learning, and automatically trades off exploration against exploitation by dynamically and automatically tuning a temperature parameter that determines the stochasticity of the policy. We show that this method achieves state-of-the-art performance on four standard benchmark environments. We then demonstrate that it can be used to learn quadrupedal locomotion gaits on a real-world Minitaur robot, learning to walk from scratch directly in the real world in two hours of training. Videos of training and the learned policy can be found on the project website³.

I. INTRODUCTION

Deep reinforcement learning can be used to automate the acquisition of controllers for a range of robotic tasks, enabling end-to-end learning of policies that map sensory inputs to low-level actions. This can be particularly appealing in the domain of robotic locomotion, where manual gait design can be difficult and highly robot-specific. If we can learn locomotion gaits from scratch directly in the real world, we can in principle acquire controllers that are ideally adapted to each robot and even to individual terrains, potentially achieving better agility, energy efficiency, and robustness. However, applying end-to-end deep reinforcement learning with general-purpose function approximators is complicated by two major challenges. The first is the large sample requirements of many deep reinforcement learning algorithms, which might require tens of thousands of trials in the real world. The second, more subtle challenge is the severe sensitivity many of these methods have to hyperparameters settings [1]. In simulation, hyperparameters can be tuned in parallel, but in the real world, this requires multiple distinct training runs, further exacerbating the already severe sample complexity challenges. Many robotic systems, especially legged robots

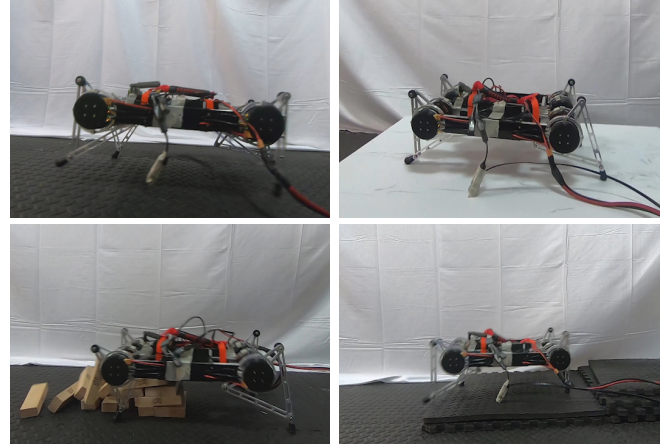


Fig. 1: Illustration of a walking gait learned in the real world. The policy is trained only on flat terrain, but due to maximum entropy training, the learned gait is stable and robust, and enables the robot to traverse obstacles that were not seen during training.

that can fall and damage themselves, simply cannot survive so many repeated trials, especially under the control of a suboptimal and partially trained policy.

In this paper, we take steps to address both of these challenges through the development of a sample-efficient deep reinforcement learning algorithm based on the principle of maximum entropy. Our aim is to devise a method that robustly trades off exploration and exploitation, while being relatively insensitive to hyperparameter settings. Our end goal is to make it feasible to learn locomotion skills directly in the real world, end-to-end, without simulated training or reliance on passive stability or low-dimensional policy representations, such that our approach is automated and broadly applicable. We build on model-free off-policy methods based on value function estimation, since such algorithms generally provide improved sample efficiency compared to on-policy algorithms [2], [3], [4], [5]. In particular, we extend the framework of maximum entropy reinforcement learning. Methods of this type, such as soft actor-critic [6] and soft Q-learning [7], can achieve state-of-the-art sample efficiency [6] and have been successfully deployed for other real-world tasks, such as robotic manipulation, where they exhibit a high degree of robustness due to entropy maximization [8]. However, maximum entropy RL algorithms are sensitive to the choice of temperature parameter, which determines the trade-off between exploration (the entropy weight) and exploitation (reward maximization). While this parameter can be viewed as part of the task, with the reward magnitude encoding the user’s preference for high rewards versus robustness, in

¹Berkeley Artificial Intelligence Research, University of California, Berkeley, {haarnoja, azhou42, svlevine}@berkeley.edu

²Google Brain, {sehoonha, jietan, gjt}@google.com

³<https://sites.google.com/view/minitaur-locomotion/>

practice this temperature is a hyperparameter that must be tuned by hand.

We devise a variant of the maximum entropy soft actor-critic algorithm [6] that removes the need to manually tune the temperature, proposing a simple and automatic gradient-based temperature tuning method that adjusts the expected entropy over the visited states to match a target value. In contrast to standard reinforcement learning, our method only controls the expected entropy over states, while the per-state entropy can still vary—a desirable property that allows the policy to automatically reduce entropy for states where acting deterministically is preferred, while still acting stochastically in other states. Although this modification is simple, we find that in practice it virtually eliminates the need for per-task hyperparameter tuning, making it practical for us to apply this algorithm to learn quadrupedal locomotion gaits directly on a real-world robotic system.

The principal contributions of our paper are the automatic temperature adjustment scheme for maximum entropy reinforcement learning algorithms, and an empirical evaluation of this algorithm on both simulated benchmark tasks and on learning real-world quadrupedal locomotion on the Minitaur robot (Figure 1). In real-world experiments, our algorithm can enable the Minitaur to learn to walk using about 400 rollouts (160,000 time steps). This is equivalent to about 2 hours of training. We also describe the details of our real-world reinforcement learning experimental setup. Furthermore, in evaluations on standard RL benchmark tasks, our method achieves state-of-the-art performance and, unlike prior state-of-the-art methods based on maximum entropy RL, can use exactly the same hyperparameters for all tasks.

II. RELATED WORK

Maximum entropy reinforcement learning optimizes policies to maximize both the expected return and the expected entropy of the policy. This framework has been used in many contexts, from inverse reinforcement learning [9] to optimal control [10], [11], [12]. Maximum a posteriori policy optimization (MPO) makes use of the probabilistic view and optimizes the standard RL objective via expectation maximization [13]. In guided policy search [14], [15], the maximum entropy distribution is used to guide policy learning towards high-reward regions. More recently, several papers have noted the connection between Q-learning and policy gradient methods in the framework of maximum entropy learning [16], [7], [17], [18]. While most of the prior model-free works assume a discrete action space, some works approximate the maximum entropy distribution with a Gaussian [19] or with a sampling network trained to draw samples from the optimal policy [7]. Although the soft Q-learning algorithm [7] has a value function and actor network, it is not a true actor-critic algorithm: the Q-function is estimating the optimal Q-function, and the actor does not directly affect the Q-function except through the data distribution. Hence, in [7] the actor network is motivated as an approximate sampler, rather than the actor in an actor-critic algorithm. Crucially, the convergence of this method hinges

on how well this sampler approximates the true posterior. In contrast, soft actor-critic can be proved to converge to the optimal policy from a given policy class, regardless of the policy parameterization [6].

Deep reinforcement learning has been used extensively to learn locomotion policies in simulation [20], [21], [22], [23] and even transfer them to real-world robots [24], but this inevitably incurs some loss of performance due to discrepancies in the simulation, and requires extensive manual modeling. Using such algorithms directly in the real world has proven challenging. Real-world applications typically make use of simple and inherently stable robots [25] or low-dimensional gait parameterizations [26], [27], [28], or both [29]. In contrast, we show we can acquire locomotion skills directly in the real world using policies based on deep networks.

III. PRELIMINARIES

Reinforcement learning aims to learn a policy that maximizes the expected sum of rewards [30]. We consider infinite-horizon Markov decision processes where the state space \mathcal{S} and action space \mathcal{A} are continuous. The agent starts at an initial state $s_0 \sim p(s_0)$. Then, the agent repeatedly samples an action a_t from a policy $\pi_\theta(a_t|s_t)$, receives a bounded reward $r(s_t, a_t)$, and transitions to a subsequent state s_{t+1} according to the Markovian dynamics $p(s_{t+1}|a_t, s_t)$ of the environment. This generates a trajectory of states and actions $\tau = (s_0, a_0, s_1, a_1, \dots)$. We denote the trajectory distribution induced by π by $\rho_\pi(\tau)$, the state-action marginal by $\rho_\pi(s_t, a_t)$ and the state marginal by $\rho_\pi(s_t)$.

Maximum entropy reinforcement learning optimizes both the expected return and the entropy of the policy. The corresponding objective can be expressed as

$$J(\pi) = \sum_{t=0}^T \mathbb{E}_{\tau \sim \rho_\pi} [r(s_t, a_t) - \alpha \log \pi(a_t|s_t)], \quad (1)$$

which incentivizes the policy to explore more widely and is more robust in practice [6]. The temperature parameter α determines the relative importance of the entropy term against the reward, and thus controls the stochasticity of the optimal policy. The maximum entropy objective differs from the standard maximum expected reward objective used in conventional reinforcement learning, though the conventional objective can be recovered in the limit as $\alpha \rightarrow 0$. We can extend the objective to infinite horizon problems by introducing a discount factor γ to ensure that the sum of expected rewards and entropies is finite [7].

One of the central challenges with the objective in (1) is that the trade-off between maximizing the return, or exploitation, versus the entropy, or exploration, is directly affected by the scale of the reward function. Unlike in conventional reinforcement learning, where the optimal policy is independent of scaling of the reward function, in maximum entropy reinforcement learning the scaling factor has to be tuned per environment, and a sub-optimal scale can drastically degrade the performance [6]. In the next section, we will

propose an algorithm that optimizes a related objective that allows us to better control the exploration-exploitation trade-off. We will first derive an theoretical algorithm for finite horizon case, and then suggest a practical algorithm for discounted, infinite horizon case based on the theory.

IV. AUTOMATING ENTROPY ADJUSTMENT FOR MAXIMUM ENTROPY RL

Instead of requiring the user to set the temperature or reward scale manually, we can automate this process by formulating a different maximum entropy reinforcement learning objective, where the entropy is treated as a constraint. The magnitude of the reward differs not only across tasks, but it also depends on the policy, which improves over time during training. Since the optimal entropy depends on this magnitude, this makes the temperature adjustment particularly difficult: the entropy can vary unpredictably both across tasks and during training as the policy becomes better. Simply forcing the entropy to a fixed value is a poor solution, since the policy should be free to explore more in regions where the optimal action is uncertain, but remain more deterministic in states with a clear distinction between good and bad actions. Instead, we formulate a constrained optimization problem where the *average* entropy of the policy is constrained, while the entropy at different states can vary. Similar approach was taken in [13], where the policy was constrained to remain close to the previous policy. We show that the dual to this constrained optimization leads to the soft actor-critic updates [6], along with an additional update for the dual variable, which plays the role of the temperature. Our formulation also makes it possible to learn the entropy with more expressive policies that can model multi-modal distributions, such as policies based on normalizing flows [31], for which no closed form expression for the entropy exists.

A. Constrained Entropy Objective

Our aim is to find a stochastic policy with maximal expected return that satisfies a minimum expected entropy constraint. Formally, we want to solve the constrained optimization problem

$$\max_{\pi_{0:T}} \mathbb{E}_{\rho_\pi} \left[\sum_{t=0}^T r(\mathbf{s}_t, \mathbf{a}_t) \right] \text{ s.t. } \mathbb{E}_{\rho_\pi} [-\log(\pi_t(\cdot | \mathbf{s}_t))] \geq \mathcal{H}, \quad (2)$$

where \mathcal{H} is a desired minimum expected entropy. Note that, for fully observed MDPs, the policy that optimizes the expected return is deterministic, so we expect this constraint to usually be tight and do not need to impose an upper bound on the entropy.

Since the policy at time t can only affect the future objective value, we can employ an (approximate) dynamic programming approach, solving for the policy backward through time. We rewrite the objective as an iterated maximization

$$\max_{\pi_0} \left(\mathbb{E}[r(\mathbf{s}_0, \mathbf{a}_0)] + \max_{\pi_1} \left(\mathbb{E}[\dots] + \max_{\pi_T} \mathbb{E}[r(\mathbf{s}_T, \mathbf{a}_T)] \right) \right),$$

subject to the constraint on entropy. Starting from the last time step, we change the constrained maximization to the dual problem. Subject to $\mathbb{E}_{\rho_\pi} [-\log(\pi_T(\cdot | \mathbf{s}_T))] \geq \mathcal{H}$,

$$\begin{aligned} \max_{\pi_T} \mathbb{E}_{(\mathbf{s}_T, \mathbf{a}_T) \sim \rho_\pi} [r(\mathbf{s}_T, \mathbf{a}_T)] = \\ \min_{\alpha_T \geq 0} \max_{\pi_T} \mathbb{E} [r(\mathbf{s}_T, \mathbf{a}_T) - \alpha_T \log \pi(\mathbf{a}_T | \mathbf{s}_T)] - \alpha_T \mathcal{H}, \end{aligned}$$

where α_T is the dual variable. We have also used strong duality, which holds since the objective is linear and the constraint (entropy) is convex function in π_T . This dual objective is closely related to the maximum entropy objective RL objective with respect to the policy. Let $\pi_T^*(\mathbf{a}_T | \mathbf{s}_T; \alpha_T)$ be the unique maximizer. We can solve for the optimal dual variable α_T^* as

$$\arg \min_{\alpha_T} \mathbb{E}_{\mathbf{s}_T, \mathbf{a}_T \sim \pi_T^*} [-\alpha_T \log \pi_T^*(\mathbf{a}_T | \mathbf{s}_T; \alpha_T) - \alpha_T \mathcal{H}]. \quad (3)$$

To simplify notation, we make use of the recursive definition of the soft Q-function

$$\begin{aligned} Q_t^*(\mathbf{s}_t, \mathbf{a}_t; \pi_{t+1:T}^*, \alpha_{t+1:T}^*) &= \mathbb{E}[r(\mathbf{s}_t, \mathbf{a}_t)] \\ &+ \mathbb{E}_{\rho_\pi} [Q_{t+1}^*(\mathbf{s}_{t+1}, \mathbf{a}_{t+1}) - \alpha_{t+1}^* \log \pi_{t+1}^*(\mathbf{a}_{t+1} | \mathbf{s}_{t+1})], \end{aligned}$$

with $Q_T^*(\mathbf{s}_T, \mathbf{a}_T) = \mathbb{E}[r(\mathbf{s}_T, \mathbf{a}_T)]$. Now, subject to the entropy constraints and again using the dual problem, we have

$$\begin{aligned} \max_{\pi_{T-1}} \left(\mathbb{E}[r(\mathbf{s}_{T-1}, \mathbf{a}_{T-1})] + \max_{\pi_T} \mathbb{E}[r(\mathbf{s}_T, \mathbf{a}_T)] \right) = \\ \max_{\pi_{T-1}} (Q_{T-1}^*(\mathbf{s}_{T-1}, \mathbf{a}_{T-1}) - \alpha_T \mathcal{H}) = \\ \min_{\alpha_{T-1} \geq 0} \max_{\pi_{T-1}} \left(\mathbb{E}[Q_{T-1}^*(\mathbf{s}_{T-1}, \mathbf{a}_{T-1})] \right. \\ \left. - \mathbb{E}[\alpha_{T-1} \log \pi(\mathbf{a}_{T-1} | \mathbf{s}_{T-1})] - \alpha_{T-1} \mathcal{H} \right) + \alpha_T^* \mathcal{H}. \end{aligned}$$

In this way, we can proceed backwards in time and recursively optimize (2).

The optimal policy $\pi_t^*(\mathbf{a}_t | \mathbf{s}_t; \alpha_t)$ for time t can now be expressed as

$$\arg \min_{\pi_t} D_{\text{KL}} \left(\pi_t \parallel \frac{1}{Z(\mathbf{s}_t)} \exp \left(\frac{1}{\alpha_t} Q_t^*(\mathbf{s}_t, \mathbf{a}_t) \right) \right), \quad (4)$$

where $Z(\mathbf{s}_t)$ is a (generally) intractable log-partition function. However, $Z(\mathbf{s}_t)$ does not depend on π_t^* , so we can ignore it for the purposes of optimizing π_t^* . This is exactly the soft policy improvement step introduced by [6], with an additional temperature parameter α_t . In contrast to [6], which shows that this update leads to an improvement in the policy, we derived it directly starting from the objective function. Note that the optimal policy at time t is a function of the dual variable α_t^* . Similarly, we can solve the optimal dual variable α_t^* after solving for Q_t^* and π_t^* :

$$\alpha_t^* = \arg \min_{\alpha_t} \mathbb{E}_{\mathbf{a}_t \sim \pi_t^*} [-\alpha_t \log \pi_t^*(\mathbf{a}_t | \mathbf{s}_t; \alpha_t) - \alpha_t \mathcal{H}]. \quad (5)$$

The solutions in (4) and (5) constitute the core of our algorithm. In theory, exactly solving these equations recursively optimizes the entropy-constrained maximum expected return objective in (2). However, to produce a practical algorithm

for real-world learning, we will need to utilize function approximators and stochastic gradient descent, as discussed in the next section.

B. Practical Algorithm

In practice, we cannot perform the optimization steps in (4) and (5) exactly. We instead parameterize a Gaussian policy with parameters ϕ and a temperature parameter, and learn the policy using stochastic gradient descent for the discounted, infinite horizon problem. We additionally use two parameterized Q-functions, with parameters θ_1 and θ_2 , as suggested in [6]. We learn the Q-function parameters as a regression problem by minimizing the following loss $J_Q(\theta_i)$:

$$\mathbb{E}_{(\mathbf{s}_t, \mathbf{a}_t, \mathbf{s}_{t+1}) \sim \mathcal{D}} \left[(Q_{\theta_i}(\mathbf{s}_t, \mathbf{a}_t) - (r(\mathbf{s}_t, \mathbf{a}_t) + \gamma V_{\theta_1, \theta_2}(\mathbf{s}_{t+1})))^2 \right] \quad (6)$$

using minibatches from a replay buffer \mathcal{D} . The value function $V_{\theta_1, \theta_2}(\mathbf{s}_t)$ is implicitly defined through the Q-functions and the policy as $\mathbb{E}_{\mathbf{a}_t \sim \pi_\phi} \left[\min_{i \in \{1, 2\}} Q_{\theta_i}(\mathbf{s}_t, \mathbf{a}_t) - \alpha \log \pi_\phi(\mathbf{a}_t | \mathbf{s}_t) \right]$. We learn a Gaussian policy by minimizing

$$J_\pi(\phi) = \mathbb{E}_{\mathbf{s}_t \sim \mathcal{D}, \mathbf{a}_t \sim \pi_\phi} \left[\alpha \log \pi_\phi(\mathbf{a}_t | \mathbf{s}_t) - \min_{i \in \{1, 2\}} Q_{\theta_i}(\mathbf{s}_t, \mathbf{a}_t) \right], \quad (7)$$

using the reparameterization trick [32]. This procedure is the same as the standard soft actor-critic algorithm [6], but with an explicit, dynamic temperature α .

To learn α , we need to minimize the dual objective in (5). This can be done by approximating dual gradient descent [33]. Dual gradient descent alternates between optimizing the Lagrangian with respect to the primal variables to convergence, and then taking a gradient step on the dual variables. While optimizing with respect to the primal variables fully is impractical, a truncated version that performs incomplete optimization (even a single gradient step) can be shown to converge under convexity assumptions [33]. While such assumptions do not apply to the case of nonlinear function approximators such as neural networks, we found this approach to still work in practice. Thus, we compute gradients for α with the following objective:

$$J(\alpha) = \mathbb{E}_{\mathbf{s}_t \sim \mathcal{D}, \mathbf{a}_t \sim \pi_\phi} [-\alpha \log \pi_\phi(\mathbf{a}_t | \mathbf{s}_t) - \alpha \mathcal{H}]. \quad (8)$$

The proposed algorithm alternates between a data collection phase and an optimization phase. In the optimization phase, the algorithm optimizes all objectives in (6) – (8) jointly. We also incorporate delayed target Q-function networks as is standard in prior work. Algorithm 1 summarizes the full algorithm, where $\hat{\nabla}$ denotes stochastic gradients.

V. COMPARATIVE EXPERIMENTS IN SIMULATION

The aim of our simulated evaluation is to evaluate whether our algorithm can achieve state-of-the-art performance across a range of different domains without tuning of hyperparameters. To that end, we evaluate our algorithm on four continuous locomotion tasks from the Gym benchmark

Algorithm 1: Soft Actor-Critic with Automatic Entropy Adjustment

```

1 Initialize function approximators parameters  $\theta_1, \theta_2, \phi$ ,
  and a global temperature coefficient  $\alpha$ .
2 for each iteration do
3   for each environment step do
4      $\mathbf{a}_t \sim \pi(\mathbf{a}_t | \mathbf{s}_t)$ 
5      $\mathbf{s}_{t+1} \sim p(\mathbf{s}_{t+1} | \mathbf{s}_t, \mathbf{a}_t)$ 
6      $\mathcal{D} \leftarrow \mathcal{D} \cup \{(\mathbf{s}_t, \mathbf{a}_t, r(\mathbf{s}_t, \mathbf{a}_t), \mathbf{s}_{t+1})\}$ .
7   end
8   for each gradient step do
9      $\theta_i \leftarrow \theta_i - \lambda \hat{\nabla}_{\theta_i} J_Q(\theta_i)$  for  $i \in \{1, 2\}$ 
10     $\phi \leftarrow \phi - \lambda \hat{\nabla}_{\phi} J_\pi(\phi)$ 
11     $\alpha \leftarrow \alpha - \lambda \hat{\nabla}_{\alpha} J(\alpha)$ 
12  end
13   $\bar{\theta}_i \leftarrow \tau \theta_i + (1 - \tau) \bar{\theta}_i$  for  $i \in \{1, 2\}$ 
14 end

```

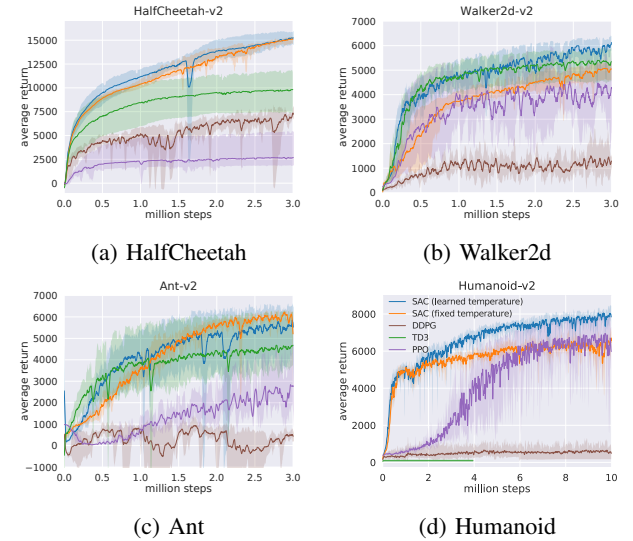
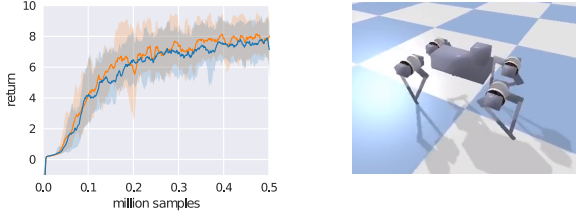


Fig. 2: (a) – (d) Standard benchmark training results. Our method (green) is able to match the state-of-the-art baseline (orange) without environment specific tuning. DDPG (blue) performs well in lower-dimensional tasks, but fails on Humanoid, which has 17 action dimensions.

suite [34], ranging from HalfCheetah with six action dimensions to Humanoid with 17-dimensional actions. We compare our method to soft actor-critic (SAC) [6] with a fixed temperature parameter that is tuned for each environment. We also compare to deep deterministic policy gradient (DDPG) [3], proximal policy optimization (PPO) [35], and twin delayed deep deterministic policy gradient algorithm [4].

All of the algorithms use the same network architecture: all of the function approximators (policy and Q-functions for SAC) are parameterized with a two-layer neural network with 256 hidden units on each layer, and we use ADAM [36] to learn the weights. For standard SAC, we tune the reward scale per environment using grid search. Poorly chosen reward scales can degrade performance drastically (see Figure 4a). For our method, we simply set the target entropy to be -1 nats



(a) Minitaur locomotion task (b) Minitaur simulation

Fig. 3: (a) Learning curves for the Minitaur environment. For our method (green), we used exactly the same hyper-parameters as we used for the benchmarks whereas for the baseline (orange), we needed to tune the reward scale. (b) Illustration of the Minitaur environment.

per action dimension (i.e., HalfCheetah has target entropy -6, while Humanoid uses -17).

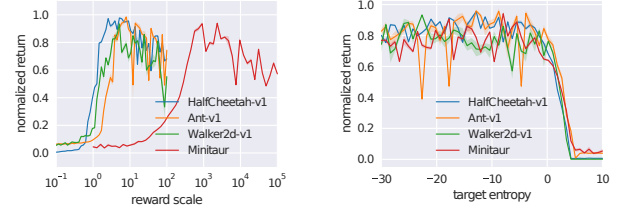
A. Comparative Evaluation

Figure 2(a) – (d) show a comparison of the algorithms. The solid line denotes the average performance over 5 random seeds, and the shaded region corresponds to the best and worst performing seeds. The results indicate that our method (blue) achieves practically identical or better performance compared to standard SAC (orange), which is tuned per environment for all environments. Overall, SAC performs better of comparably to the other baselines, DDPG, TD3, and PPO.

We also applied our method to a simulated Minitaur environment (Figure 3). Note that the purpose of testing in the simulated Minitaur environment is to demonstrate the insensitivity of hyperparameters of our algorithm. We do not use the policy learned in simulation in our real-world experiments (Section VI). This Minitaur environment is more realistic than the benchmark environments, as it has been carefully system identified to match a real robotic platform so that the learned controller in simulation could be transferred on the real Minitaur robot [24]. This it is more representative of an actual use case of model-free reinforcement learning in robotics. Figure 3(a) compares the learning curve of our method (green), with exactly the same parameters used in the benchmarks, to standard SAC (orange) with tuned reward scale. Note that in order to obtain the baseline comparison, we had to collect approximately an order of magnitude more samples from the environment to tune the hyperparameter, which is not shown in the figure.

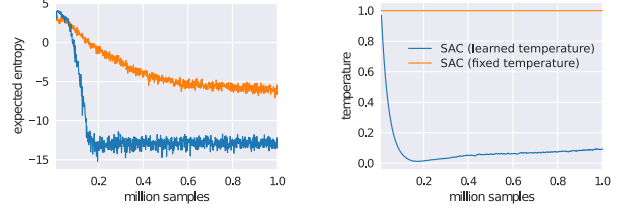
B. Sensitivity Analysis

In this section, we study the sensitivity of our method to reward scale and the value of the target entropy. Both maximum entropy RL algorithms [6] and standard RL algorithms [1] can be very sensitive to the scale of the reward function. In the case of maximum entropy RL, this scale directly affects the trade-off between reward maximization and entropy maximization [6]. We evaluate sensitivity on the HalfCheetah, Ant, and Walker tasks, as well as the simulated Minitaur robot. Figure 4a shows the normalized return for a range of reward scale values. All benchmark environments achieve good performance for about the same



(a) Reward scale (b) Target entropy

Fig. 4: Average normalized performance over the last 100k samples on a range of environments. (a) Performance of standard SAC as a function of reward scale, and (b) performance of the proposed method as a function of target entropy. Our method is substantially less sensitive to the choice of the hyper-parameter controlling the stochasticity of the policy.



(a) Entropy (b) Temperature

Fig. 5: Comparison our method and standard SAC in terms of entropy and temperature on HalfCheetah. The target entropy for learning the temperature of SAC is -13 in this case.

range of values, between 1 to 10. On the other hand, the simulated Minitaur requires roughly two orders of magnitude larger reward scale to work properly. This result indicates that, while standard benchmarks offer high variability in terms of task dimensionality, they are homogeneous in terms of other characteristics, and testing only on the benchmarks might not generalize well to seemingly similar tasks designed for different purposes. This suggests that the good performance of our method, with the same hyperparameters, on both the benchmark tasks and the Minitaur task accurately reflects its generality and robustness. Figure 4b compares the sensitivity of our method to the target entropy value on the same set of tasks. In this case, the range of good target entropy values is essentially the same for all environments, making hyper-parameter tuning substantially less laborious. It is also worth noting that this range is very large, suggesting that our algorithm is relatively insensitive to the choice of this hyperparameter.

Next, we compared how the entropy and temperature evolve during training. Figure 5a compares the entropy (estimated as an expected negative log probability over a minibatch) on HalfCheetah for SAC with fixed temperature (orange) and our method (blue), which uses a target entropy of -13. The figure clearly indicates that our algorithm is able to match the target entropy in a relatively small number of steps. On the other hand, regular SAC has a fixed temperature parameter and thus the entropy slowly decreases as the Q-function increases. Figure 5b compares the temperature parameter of the two methods. Our method (blue) actively adjusts the temperature,

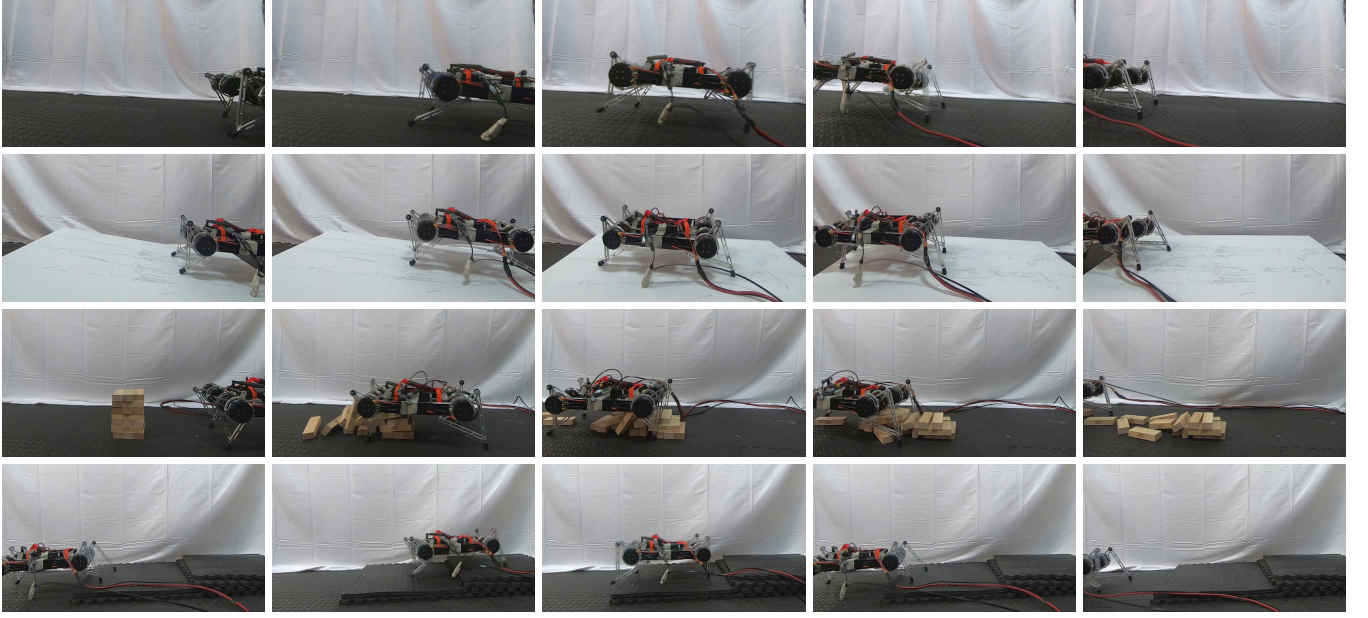


Fig. 6: We trained the Minitaur robot to walk on flat terrain (first row) in about two hours. At test time, we introduced obstacles, including a slope, wooden blocks, and steps, which were not present at training time, and the learned policy was able to generalize to the unseen situations without difficulty (other rows). Videos are available at sites.google.com/view/minitaur-locomotion/.

particularly in the beginning of training when the Q-values are small and the entropy term dominates in the objective. The temperature is quickly pulled down so as to make the entropy to match the target.

VI. QUADRUPEDAL LOCOMOTION IN THE REAL WORLD

In this section, we describe an application of our method to learn walking gaits directly in the real world. We use the Minitaur robot, a small-scale quadruped with eight direct-drive actuators [37]. Each leg is controlled by two actuators that allow it to move in the sagittal plane. The Minitaur is equipped with motor encoders that measure the motor angles and an IMU that measures orientation and angular velocity of Minitaur’s base. The action space are the swing angle and the extension of each leg, which are then mapped to desired motor positions and tracked with a PD controller [24]. The observations include the motor angles as well as roll and pitch angles and angular velocities of the base. We exclude yaw since it is unreliable due to drift and irrelevant for the walking task. Note that latencies in the hardware and contact dynamics make the system non-Markovian, which can significantly degrade learning performance. We therefore construct the state out of the current and past five observations and actions. The reward function rewards large forward velocity, which is estimated using a motion capture system, and penalizes large angular accelerations, computed via finite differences using the last three actions. We also found it necessary to penalize for large pitch angles and for extending the front legs under the robot, which we found to be the most common failure cases that would require manual resets. We parameterize the policy and the value functions with feed-forward neural networks with two hidden-layers and 256 neurons per layer.

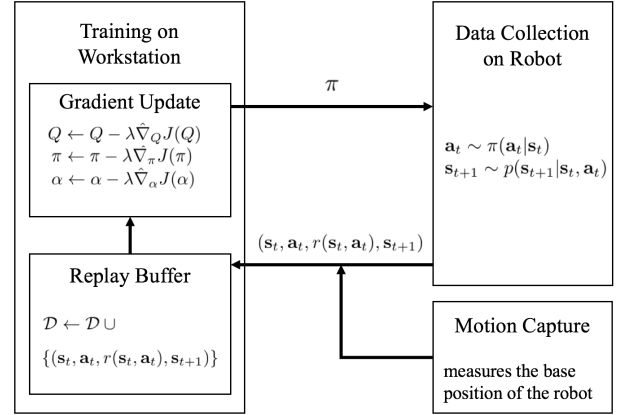


Fig. 7: The training pipeline runs the training and data collection asynchronously and seamlessly across multiple machines.

We developed a semi-automatic robot training pipeline (Figure 7) that consists of two parallel components: training and data collection. These jobs run asynchronously on two different computers. The training process runs on a workstation, which updates the neural networks and periodically downloads the latest data from the robot and uploads the latest policy to the robot. On the robot, the on-board NVIDIA Jetson TX2 runs the data collection job, which executes the policy, collects the trajectory, and uploads the data to the workstation through Ethernet. Once the training is started, minimal human intervention is needed, except for the need to reset the robot state if it falls or drifts too far from the initial state.

Quadrupedal locomotion presents substantial challenges for real-world reinforcement learning. The robot is underactuated,

and must therefore delicately balance contact forces on the legs to make forward progress. An untrained policy can lose balance and fall, and too many falls will eventually damage the robot, making sample-efficient learning essential. Our method successfully learns to walk from 160k environment steps, or approximately 400 episodes with maximum length of 500 steps, which amounts to approximately 2 hours of real-world training time. We have included videos of the training and evaluation on our project website¹.

However, in the real world, the utility of a locomotion policy hinges critically on its ability to generalize to different terrains and obstacles. Although we trained our policy only on flat terrain, as illustrated in Figure 6 (first row), we then tested it on varied terrains and obstacles (other rows). Because soft actor-critic learns robust policies due to entropy maximization at training time, the policy can readily generalize to these perturbations without any additional learning. The robot is able to walk up and down a slope (first row), ram through an obstacle made of wooden blocks (second row), and step down stairs (third row) without difficulty, despite not being trained in these settings. To our knowledge, this experiment is the first example of a deep reinforcement learning algorithm learning underactuated quadrupedal locomotion directly in the real world without any simulation or pretraining.

VII. DISCUSSION AND FUTURE WORK

We present an automatic entropy adjustment scheme for maximum entropy reinforcement learning and apply it to soft actor critic, resulting in an algorithm which is sample-efficient and stable with respect to hyperparameter settings, thus making it well-suited for learning quadrupedal locomotion gaits end-to-end directly on a real-world Minitaur robot. Our method is based on a dual formulation of an entropy-constrained reinforcement learning objective, which builds on the framework of maximum entropy RL but introduces an explicit trade-off between exploration and exploitation that is invariant to reward magnitude and much easier to set in practice. The same entropy constraint value works well across all of the benchmark tasks we tested, where our method achieves state-of-the-art efficiency, and on both the simulated and real robotic walking tasks, where the temperature did not require any modification or tuning. Our real-world experiments indicate that soft actor-critic is robust and sample efficient enough for robotic tasks learned directly in the real world. To our knowledge, these results represent the first evaluation of deep reinforcement learning for real-world training of underactuated walking skills with a quadrupedal robot.

REFERENCES

- [1] P. Henderson, R. Islam, P. Bachman, J. Pineau, D. Precup, and D. Meger, "Deep reinforcement learning that matters," in *Conference on Artificial Intelligence (AAAI)*. AAAI, 2018.
- [2] H. V. Hasselt, "Double Q-learning," in *Advances in Neural Information Processing Systems (NeurIPS)*, 2010, pp. 2613–2621.
- [3] T. P. Lillicrap, J. J. Hunt, A. Pritzel, N. Heess, T. Erez, Y. Tassa, D. Silver, and D. Wierstra, "Continuous control with deep reinforcement learning," *arXiv preprint arXiv:1509.02971*, 2015.
- [4] S. Fujimoto, H. van Hoof, and D. Meger, "Addressing function approximation error in actor-critic methods," in *International Conference on Machine Learning (ICML)*, 2018.
- [5] O. Nachum, M. Norouzi, G. Tucker, and D. Schuurmans, "Smoothed action value functions for learning gaussian policies," *arXiv preprint arXiv:1803.02348*, 2018.
- [6] T. Haarnoja, A. Zhou, P. Abbeel, and S. Levine, "Soft actor-critic: Off-policy maximum entropy deep reinforcement learning with a stochastic actor," in *International Conference on Machine Learning (ICML)*, 2018.
- [7] T. Haarnoja, H. Tang, P. Abbeel, and S. Levine, "Reinforcement learning with deep energy-based policies," in *International Conference on Machine Learning (ICML)*, 2017, pp. 1352–1361.
- [8] T. Haarnoja, V. Pong, A. Zhou, M. Dalal, P. Abbeel, and S. Levine, "Composable deep reinforcement learning for robotic manipulation," in *International Conference on Robotics and Automation (ICRA)*. IEEE, 2018.
- [9] B. D. Ziebart, A. L. Maas, J. A. Bagnell, and A. K. Dey, "Maximum entropy inverse reinforcement learning," in *AAAI Conference on Artificial Intelligence (AAAI)*, 2008, pp. 1433–1438.
- [10] E. Todorov, "General duality between optimal control and estimation," in *Conference on Decision and Control (CDC)*. IEEE, 2008, pp. 4286–4292.
- [11] M. Toussaint, "Robot trajectory optimization using approximate inference," in *International Conference on Machine Learning (ICML)*. ACM, 2009, pp. 1049–1056.
- [12] K. Rawlik, M. Toussaint, and S. Vijayakumar, "On stochastic optimal control and reinforcement learning by approximate inference," in *Robotics: Science and Systems (RSS)*, 2012, pp. 3052–3056.
- [13] A. Abdolmaleki, J. T. Springenberg, Y. Tassa, R. Munos, N. Heess, and M. Riedmiller, "Maximum a posteriori policy optimisation," *arXiv preprint arXiv:1806.06920*, 2018.
- [14] S. Levine and V. Koltun, "Guided policy search," in *International Conference on Machine Learning (ICML)*, 2013, pp. 1–9.
- [15] S. Levine, C. Finn, T. Darrell, and P. Abbeel, "End-to-end training of deep visuomotor policies," *Journal of Machine Learning Research*, vol. 17, no. 39, pp. 1–40, 2016.
- [16] B. O'Donoghue, R. Munos, K. Kavukcuoglu, and V. Mnih, "Pqg: Combining policy gradient and q," *arXiv preprint arXiv:1611.01626*, 2016.
- [17] O. Nachum, M. Norouzi, K. Xu, and D. Schuurmans, "Bridging the gap between value and policy based reinforcement learning," in *Advances in Neural Information Processing Systems (NeurIPS)*, 2017, pp. 2772–2782.
- [18] J. Schulman, P. Abbeel, and X. Chen, "Equivalence between policy gradients and soft Q-learning," *arXiv preprint arXiv:1704.06440*, 2017.
- [19] O. Nachum, M. Norouzi, K. Xu, and D. Schuurmans, "Trust-PCL: An off-policy trust region method for continuous control," in *International Conference on Learning Representations (ICLR)*, 2018.
- [20] N. Heess, S. Sriram, J. Lemmon, J. Merel, G. Wayne, Y. Tassa, T. Erez, Z. Wang, A. Eslami, M. Riedmiller *et al.*, "Emergence of locomotion behaviours in rich environments," *arXiv preprint arXiv:1707.02286*, 2017.
- [21] Z. Xie, G. Berseth, P. Clary, J. Hurst, and M. van de Panne, "Feedback control for cassie with deep reinforcement learning," *arXiv preprint arXiv:1803.05580*, 2018.
- [22] X. B. Peng, G. Berseth, and M. Van de Panne, "Terrain-adaptive locomotion skills using deep reinforcement learning," *ACM Transactions on Graphics (TOG)*, vol. 35, no. 4, p. 81, 2016.
- [23] G. Berseth, C. Xie, P. Cernek, and M. Van de Panne, "Progressive reinforcement learning with distillation for multi-skilled motion control," *International Conference on Learning Representations (ICLR)*, 2018.
- [24] J. Tan, T. Zhang, E. Coumans, A. Iscen, Y. Bai, D. Hafner, S. Bohez, and V. Vanhoucke, "Sim-to-real: Learning agile locomotion for quadruped robots," in *Robotics: Science and Systems (RSS)*, 2018.
- [25] S. Ha, J. Kim, and K. Yamane, "Automated deep reinforcement learning environment for hardware of a modular legged robot," in *International Conference on Ubiquitous Robots (UR)*. IEEE, 2018, pp. 348–354.
- [26] N. Kohl and P. Stone, "Policy gradient reinforcement learning for fast quadrupedal locomotion," in *International Conference on Robotics and Automation*, vol. 3. IEEE, 2004, pp. 2619–2624.

¹<https://sites.google.com/view/minitaur-locomotion/>

- [27] R. Calandra, A. Seyfarth, J. Peters, and M. P. Deisenroth, "Bayesian optimization for learning gaits under uncertainty," *Annals of Mathematics and Artificial Intelligence*, vol. 76, no. 1-2, pp. 5–23, 2016.
- [28] A. Rai, R. Antonova, S. Song, W. Martin, H. Geyer, and C. G. Atkeson, "Bayesian optimization using domain knowledge on the ATRIAS biped," *arXiv preprint arXiv:1709.06047*, 2017.
- [29] R. Tedrake, T. W. Zhang, and H. S. Seung, "Learning to walk in 20 minutes," in *Proceedings of the Fourteenth Yale Workshop on Adaptive and Learning Systems*, vol. 95585. Yale University New Haven (CT), 2005, pp. 1939–1412.
- [30] R. S. Sutton and A. G. Barto, *Reinforcement learning: An introduction*. MIT press Cambridge, 1998, vol. 1.
- [31] T. Haarnoja, K. Hartikainen, P. Abbeel, and S. Levine, "Latent space policies for hierarchical reinforcement learning," in *International Conference on Machine Learning (ICML)*, 2018.
- [32] D. P. Kingma and M. Welling, "Auto-encoding variational bayes," *arXiv preprint arXiv:1312.6114*, 2013.
- [33] S. Boyd and L. Vandenberghe, *Convex optimization*. Cambridge university press, 2004.
- [34] G. Brockman, V. Cheung, L. Pettersson, J. Schneider, J. Schulman, J. Tang, and W. Zaremba, "OpenAI Gym," *arXiv preprint arXiv:1606.01540*, 2016.
- [35] J. Schulman, F. Wolski, P. Dhariwal, A. Radford, and O. Klimov, "Proximal policy optimization algorithms," *arXiv preprint arXiv:1707.06347*, 2017.
- [36] D. Kingma and J. Ba, "Adam: A method for stochastic optimization," in *International Conference for Learning Presentations (ICLR)*, 2015.
- [37] G. D. Kenneally, A. De, and D. E. Koditschek, "Design principles for a family of direct-drive legged robots," *IEEE Robotics and Automation Letters*, vol. 1, no. 2, pp. 900–907, 2016.